Drug Design, Development and Therapy

Dovepress
Taylor & Francis Group

Open Access Full Text Article

ORIGINAL RESEARCH

Oleanolic Acid Cubic Liquid Crystal Nanoparticle-Based Thermosensitive Gel Attenuates Depression Symptoms in Chronic Unpredictable Mild Stress Rats

Zhiqi Shi[1,2]*, Qing Wang[1]*, Qing Li[1,3], Fan Jia[1,3], Weifeng Xu[1]

[1]Wuxi Affiliated Hospital of Nanjing University of Chinese Medicine, Wuxi, Jiangsu, People's Republic of China; [2]Liangxi District Hospital of Traditional Chinese Medicine, Wuxi, Jiangsu, People's Republic of China; [3]Wuxi Institute of Traditional Chinese Medicine, Wuxi, Jiangsu, People's Republic of China

*These authors contributed equally to this work

Correspondence: Zhiqi Shi, Chinese Medicine Research Department, Wuxi, Jiangsu, 214071, People's Republic of China, Tel +86 510-82725693, Email shi_mars@foxmail.com; Weifeng Xu, Drug Clinical Trial Facility Office, Wuxi, Jiangsu, 214071, People's Republic of China, Tel +86 510-82725693, Email 13585028501@163.com

Purpose: Major depressive disorder (MDD) is a global health concern. Studies have demonstrated that oleanolic acid (OA) has a regulatory effect on MDD. However, OA is poorly soluble, has low oral bioavailability, and faces challenges in crossing the blood-brain barrier. In this study, building upon a previous formulation of OA cubic liquid crystal nanoparticles (OA-LCNP), we combined nanoparticles with a thermosensitive gel for nasal administration and investigated the pharmacological effects of OA-LCNP thermosensitive gel (OANG) on depression. This study aimed to evaluate the effects of OANG on depression symptoms in rats.

Methods: OANG was prepared using Poloxamer F127 and F68 as the gel matrix, and the ratios of F127 and F68 were investigated. The pharmacokinetics of OANG was studied in rats, and OA content was determined using liquid chromatography-mass spectrometry (LC-MS). The pharmacological effects of OANG on depression were evaluated in chronic unpredictable mild stress (CUMS) model rats.

Results: The phase transition temperature of the gel was 34°C, and the release of OA from OANG was slow according to the Higuchi kinetic equation. The AUC_{0-t} of brain tissue after nasal OANG administration was 1.21 times that observed after intravenous administration. Additionally, the brain-targeting efficiency and nasal-brain direct transfer were 29.91% and 9.44% higher, respectively, than those observed after intravenous administration, indicating the brain-targeting capability of the OANG delivery system. Network pharmacological analysis revealed that the anti-depressant effects may be linked to neuroactive ligand-receptor interactions, the PPAR signaling pathway, and efferocytosis signaling pathways. Experimental results from CUMS rats showed that the gel significantly affected interleukin (IL)-4, IL-6, acetylcholinesterase, acetylcholine, 5-hydroxytryptamine, and brain-derived neurotrophic factor, and improved depression-like behavior in rats, as measured by sucrose preference, forced swimming, and box shuttle tests.

Conclusion: The OANG nasal drug delivery system has specific brain-targeting properties and exerts anti-depressant effects.

Keywords: oleanolic acid, cubic liquid crystal nanoparticles, drug delivery systems, major depressive disorder, chronic unpredictable mild stress

Introduction

Major depressive disorder (MDD) is a prevalent condition worldwide.[1] Studies have shown that the lifetime prevalence rates of depressive disorders range from 6.1% to 9.5%.[2] Depression can be life-threatening, with a substantial economic burden. Depressive disorders are not only seen in psychiatric clinics but also often coexist with other medical and surgical conditions. According to statistics, 22–33% of patients admitted to internal medicine are diagnosed with depressive disorders.[3] Chronic diseases, such as heart disease, cancer, chronic lung disease, and stroke, markedly

Received: 5 September 2024
Accepted: 20 January 2025
Published: 1 February 2025

increase the incidence of depressive disorders, highlighting the urgent need for new anti-depressant drugs with high efficacy and fewer side effects.[4]

Oleanolic acid (OA) is an odorless and tasteless pentacyclic triterpenoid with many pharmacological effects, including liver protection, enzyme-lowering, lipid-lowering, anti-inflammatory, antiviral, immune enhancement, platelet aggregation inhibition, hypoglycemic, anti-mutagenic, and anticancer properties.[5] OA tablets have a 94.4% efficacy rate for acute viral hepatitis and are commonly used as liver-protective drugs in clinical practice.[6] Recently, the anti-depressant pharmacological effects of OA have been discovered and have gradually attracted increasing attention. One study demonstrated that OA produces antidepressant-like effects in mice exposed to chronic stress, likely through SGK1 downregulation.[7] Kong et al also found that OA could improve depression-like behavior induced by maternal separation, including the open field and forced swimming tests, with enhanced hippocampal microglia activation and decreased tumor necrosis factor (TNF)-α expression.[8] Furthermore, a 3-week OA treatment alleviated chronic unpredictable mild stress (CUMS)-induced hedonic and anxiogenic behaviors.[9]

However, OA has very poor solubility, resulting in low dissolution, poor gastrointestinal absorption, and low bioavailability, classifying it into the fourth category according to the biopharmaceutical classification system.[10] Currently, the dosage forms used to improve OA bioavailability include liposomes, nanoparticles, and solid dispersions. In our previous study, OA bioavailability was significantly improved by preparing OA lipid cubic liquid crystal nanoparticles (LCNP).[11] However, studies on OA nanoparticles and thermosensitive gels for nasal administration have not yet been reported. This study aimed to use Poloxamer F127 and F68 as carrier materials to prepare a thermosensitive nasal gel (NG) and further evaluate the pharmacokinetics and brain-targeting anti-depressant efficacy of OA-LCNP thermosensitive gel (OANG).

Materials and Methods

Animals

All rats were obtained from Spiff (Suzhou) Biotechnology Co., Ltd., Jiangsu Province, China (Animal Production License of Jiangsu Province: SCXK-2022-0006). All procedures were approved by the Experimental Animal Care and Use Committee of the Wuxi TCM Hospital (Approval Number: 2024A003-01) and conducted in accordance with the Guide for the Care and Use of Laboratory Animals (NIH Publication No. 85–23, Revised 1996).

Materials

OA was purchased from Shanghai Yuanyet Biotechnology Co., Ltd. (Shanghai, China). Clomipramine hydrochloride tablets were obtained from Xuzhou Enhua Pharmaceutical Group Co., Ltd. (Xuzhou, China). Polyethylene glycol (PEG)-2000, Poloxamer F127, and F68 were purchased from Sigma-Aldrich Co., Ltd. (Shanghai, China). Sodium dodecyl sulfate (SDS) and phytantriol were purchased from Shanghai Aladdin Biochemical Technology Co., Ltd. (Shanghai, China). Isoflurane was obtained from Lunambet Pharmaceutical Co., Ltd. (Linyi, China). 5-hydroxytryptamine (5-HT), interleukin (IL)-1β, IL-4, IL-6, acetylcholinesterase (AChE), acetylcholine (ACh), and brain-derived neurotrophic factor (BDNF) kits were acquired from Jiangsu Kaiji Biological Co., Ltd. (Nanjing, China). Ultrapure water was obtained using a Milli-Q purification system (Millipore, Burlington, Massachusetts, USA). Acetonitrile and methanol (liquid chromatography-mass spectrometry [LC-MS] grade) were purchased from Merck (New Jersey, Germany). Gentiopicrosides were obtained from the National Institute for Food and Drug Control (Beijing, China). All materials were used as received.

OA-LCNP Preparation

LCNPs were prepared using the precursor method, as previously described.[11] Phytantriol (1.6 g) and OA (0.8 g) were dissolved in absolute ethanol (2.5 mL) and sonicated at 80% power for 30 min. The organic phase was added dropwise to the aqueous phase (20 mL) containing the stabilizer F127 under agitation to form a crude dispersion, which was then sonicated in pulsed mode (0.5 s pulse interrupted by 0.5 s pause) at 40% of maximum power for 10 min to produce a milky dispersion and reduce particle size.

OANG Preparation

The OA-LCNP solution (1.5 g) was accurately weighed into a bottle. Subsequently, 0.1 g of Poloxamer F68 and 0.4 g of F127 were evenly dispersed onto the nanoparticle solution and refrigerated at 4°C overnight until the Poloxamer samples were fully expanded and completely dissolved to obtain a uniform solution.[12] PEG-2000 (1% of the total weight of the gel) was then added.

Observation of Gelling Temperature and Condition

The gelation temperature of the gel was determined using the inversion method (Figure 1).[13] Poloxamer solution (2 mL) was added to a Cillin bottle, which was then placed in a water bath and slowly heated at 1°C/min from room temperature (25°C). The bottle was quickly removed at every 1°C increase, and the liquid flow was observed by tilting the bottle at

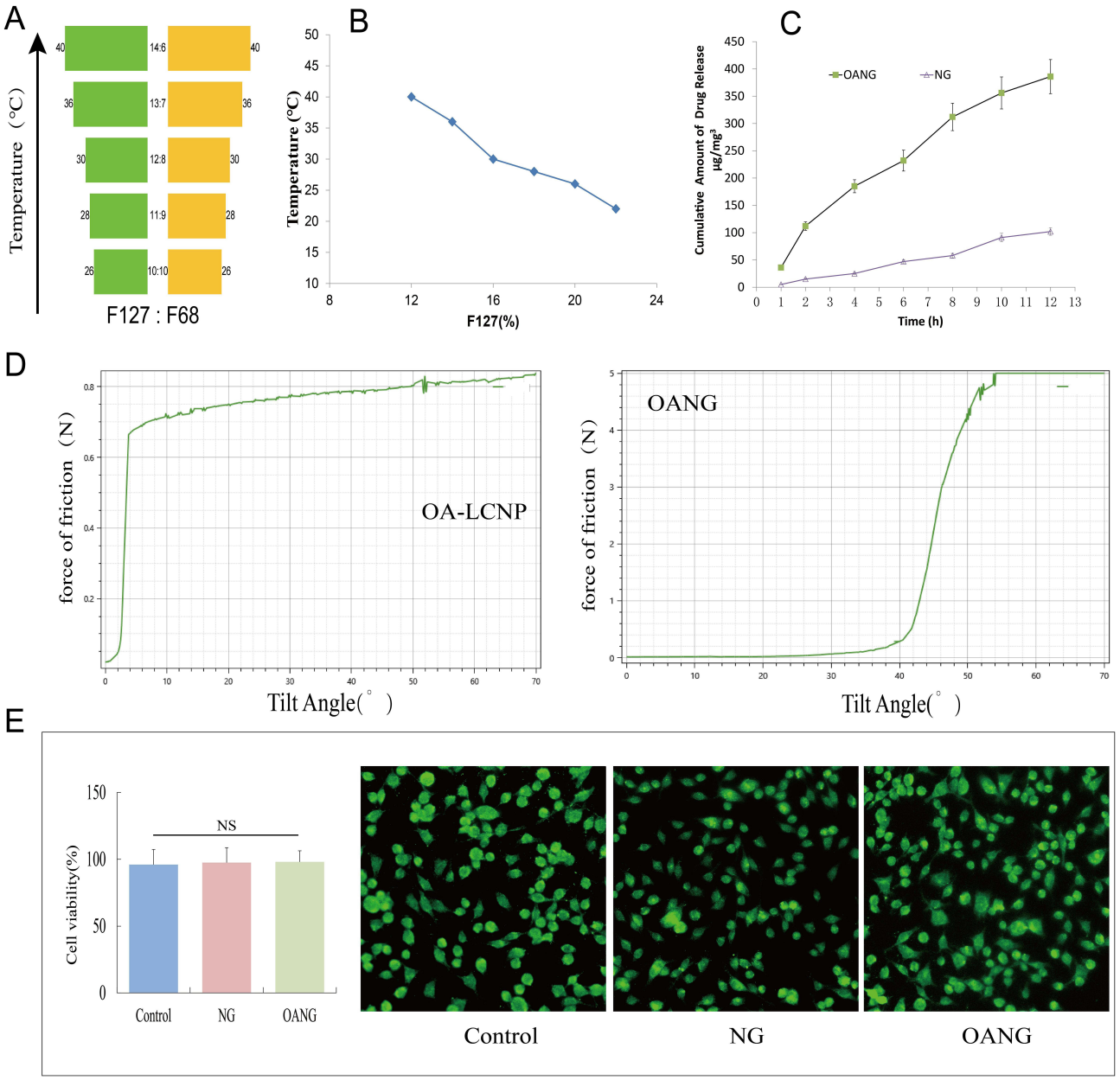

Figure 1 Results of in vitro OA evaluation. (**A**) Results of gel temperature and F127 to F68 ratio; (**B**) Results of gel temperature and F127 ratio study; (**C**) Transdermal test results (n = 3); (**D**) Rheological performance test of OA-LCNP and OANG; (**E**) Cellular viability on different hydrogels (n = 5) and staining of rat nasal mucosa cells incubated on the hydrogels.

https://doi.org/10.2147/DDDT.S484567

a 45° angle. When the liquid in the inverted bottle stopped flowing and remained stationary for 30 seconds, the solution had completely formed a gel, and the temperature at that time was recorded as the gelation temperature. Each sample was measured three times, and the average temperature was recorded.

Rheological Study

The rheological study of OANG was performed using the friction coefficient stripping test (X810, Jinan Saicheng Electronic Technology Co., Ltd.). During the test, the temperature and tilt of the observation table were set to 35 °C and 30°, respectively. Subsequently, samples (OA-LCNP and OANG, 2 g) were placed on the surface of the observation table The table temperature was gradually cooled to 25°C, and the friction coefficient was measured. An increase in the friction coefficient value indicates rapid friction between the sample and the table surface as the sample flows.[14]

Differential Scanning Calorimetry (DSC) Studies

OA raw material, OANG, and its physical mixture were evenly placed into a crucible for DSC analysis (Shanghai Hengjiu Electric Appliance Co., Ltd., China). Test conditions: heating rate was 10 °C/min, scanning range was 25–100 °C; sample atmosphere was nitrogen, and the flow rate was 50 mL/min.[15]

Infrared Spectroscopy (IR) Study

The OA raw material, OANG, and the physical mixture were ground with appropriate amounts of potassium bromide, mixed evenly, and pressed into tablets. The Fourier infrared spectrum was scanned in the wavelength range of 400–4000 cm^{-1} (Shimadzu IRTracer-100, Japan), and the corresponding spectra were recorded.[16]

Transmission Electron Microscopy (TEM) Photographing

The samples were observed directly using an F200 field-emission transmission electron microscope (JEOL Ltd., Tokyo, Japan). A carrier grid was held with tweezers and immersed in the solution to collect the droplets. After the droplets on the supporting film were fully dried, the samples were observed under the electron microscope. The nanoparticle morphology was examined at an accelerating voltage of 120 kV.[17]

In vitro MTT Study

The direct contact method was used to determine the cytocompatibility of OANG with primary nasal epithelial cells. Sterile phosphate-buffered saline (PBS) was prepared using UV irradiation at 254 nm for 30 min. The cells in each 96-well plate (1×10^4 cells/well) were coated with 100 μL of OANG and further co-cultured for 48 h. Cell viability was measured at 490 nm using the standard MTT assay.[18]

Drug Permeation Studies of OANG

Drug permeation measurements were performed using a Franz diffusion cell to evaluate the OA release profile, as previously described.[11] OANG was placed in a 50 mL centrifuge tube and heated at 37°C for 10 min to ensure full confluence. The gel was then added to the drug delivery tank for even distribution on the rat skin surface. Artificial nasal fluid (7 mL) was added to the receiving tank and maintained at 35°C, with a magnetic stirring speed of 200 rpm. Samples were obtained at 1, 2, 4, 6, 8, 10, and 12 h, and isovolumetric artificial nasal fluid was added. Artificial nasal fluid was composed of 400 mM Na^+, 140 mM K^+, and 4 mM Ca^{2+}, respectively.[19] The obtained solution was filtered through a 0.45 μm membrane, and the drug content in the sample was determined by high-performance liquid chromatography, as previously described.[11]

OANG Pharmacokinetic Study

Animals and Grouping

Male Sprague-Dawley (SD) rats (110, 180±20 g) were housed in a temperature-controlled room on a 12-h light-dark cycle with free access to standard chow and tap water. After 1 week of adaptive feeding, the rats were randomly divided into two groups: 55 rats in each of the OANG and intravenous administration (I.V.) groups. Five animals were taken at

each time interval for both the OA and OANG groups. Due to their large size and strong mobility, rats may struggle during drug administration, which may lead to bleeding caused by scratching the nasal mucosa with the drug delivery device. The rats were anesthetized with isoflurane before administration, placed in a supine position, and regained consciousness approximately 3 min after anesthesia.

The OANG (50 mg/kg) was administered to rats in the OANG group. The I.V. group received OA (50 mg/kg) directly through the tail vein (I.V.). Plasma and brain tissues were collected at 15, 30, and 45 min, and 1.0, 2.0, 4.0, 6.0, 8.0, 10.0, 12.0, and 24.0 h after administration (n = 5).

Brain Tissue and Blood Sample Preparation

The rats were anesthetized with 2% pentobarbital sodium (80 mg/kg, administered intraperitoneally). Abdominal aortic blood was collected, centrifuged at 5000 rpm for 15 min, and the supernatant was obtained and stored at −80°C. Subsequently, the rats were euthanized by decapitation under anesthesia. A comprehensive death assessment was performed by observing signs such as breathing, heartbeat, pupil response, and nerve reflexes (no chest fluctuation, eyelid blanching, and visual response). Following death confirmation, brain tissues were extracted on an ice plate, PBS buffer was added at a 1:9 ratio, homogenized for 10 min at 4°C, centrifuged at 10,000 rpm for 10 min, and the supernatant was collected and stored at −80°C.

Preparation of Reference Products and Internal Standard Solutions

OA and gentiopicroside (internal standard) were used as control products, dissolved and diluted with 80% methanol (28.6 and 27.26 μg/mL concentrations, respectively), and stored at 4°C.

Sample Pretreatment

Rat serum (200 μL) and brain tissue supernatants were added to 100 μL of the internal standard solution and mixed well. Subsequently, methanol (1 mL) was added, the mixture was swirled for 2 min, centrifuged at 10,000 rpm for 15 min, and the supernatant was obtained. The residue was transferred into another test tube, and an additional 1.5 mL of methanol was added to the precipitate, swirled for 2 min, centrifuged for 15 min at 10,000 rpm, and the supernatant was collected again. The two supernatants were combined and dried at −40°C in a vacuum, and the residue sample was obtained. Before measurement, 500 μL of 50% methanol was added to redissolve the freeze-dried residue using a centrifuge concentrator, swirled again, centrifuged for 10 min at 12,000 rpm, and the supernatant was collected for analysis.

OA Content Determination in Rat Serum and Brain Tissue Using Ultra-Performance Liquid Chromatography-Tandem Mass Spectrometry[20]

Chromatographic conditions: ACQUITY UPLC-BEH-C18 column (Part Number: 186002350, 100 mm × 2.1 mm, 1.7 μm). Mobile phase: 0.1% formic acid (A) and acetonitrile (B) by gradient elution (0–10 min, 80% A: 20% B; 10–20 min, 80–70% A: 20–30% B; 20–25 min, 70–60% A: 30–70% B; 25–26 min, 60–5% A: 70–95% B; 26–34 min, 5% A:95% B; 34–35 min, 5–80% A:95–20% B; 35–37 min, 80% A:20% B). Flow rate: 0.3 mL/min; column temperature: 40°C; sample volume: 2 μL.

Mass Spectrum Condition

Negative ion scanning mode (ESI-); scanning mode: multiple reaction monitoring; ion source temperature: 150°C; solvent removal temperature: 500°C; cone-hole gas flow rate: 150 L/h; desolvation gas flow rate: 800 L/h; impact gas flow rate: 0.25 mL/min; OA m/z: 455.8–396.3, internal standard (gentiopicroside) m/z: 355.0–149.2; cone-hole voltage: OA (60 V), gentiopicroside (60 V); collision energy: OA (20 V), gentiopicroside (18 V).

Data Processing and Statistical Analysis

All data are expressed as the mean ± standard deviation. Pharmacokinetic analysis was performed using the DAS 2.0 software with a non-atrioventricular model. Absolute bioavailability (F), brain targeting efficiency (BTE), and the percentage of nasal-brain direct transfer (NDT) were calculated to evaluate brain targeting efficiency.[19,21] Statistical comparison of pharmacokinetic data was performed with an unpaired Student's *t*-test using SPSS 21.0 (IBM Corp., Armonk, NY, USA), and $p < 0.05$ was considered statistically significant.[22]

$$F = \frac{AUC_{nasal}}{AUC_{vein}} \times 100\%$$

$$BTE = \frac{(\mathrm{AUC_{brain}}/\mathrm{AUC_{serum}})_{\mathrm{nasal}}}{(AUC_{brain}/AUC_{serum})_{vein}} \times 100\%$$

$$NDT = \frac{(AUC_{brain})_{nasal} - \frac{(AUC_{brain})_{vein}}{(AUC_{serum})_{vein}} \times (AUC_{serum})_{nasal}}{(AUC_{brain})_{nasal}} \times 100\%$$

OANG Pharmacological Study

Animals and Grouping

Male SD rats (60, 180 ± 20 g) were divided into six groups: normal, model, low-concentration OANG, high-concentration OANG, clomipramine hydrochloride, and blank gel matrix. All rats were housed in a temperature-controlled room under a 12-h light-dark cycle with free access to standard chow and tap water. After 1 week of adaptive feeding, the rats were randomly assigned to six groups (n = 10 per group): group 1, rats without treatment (normal); group 2, model group without administration (model); group 3, OANG low-concentration group (OANG 25 mg/kg per day, [OANG-L]); group 4, high-concentration OANG group (OANG 50 mg/kg per day, [OANG-H]); group 5, clomipramine hydrochloride group (60 mg/kg per day, [CH]); and group 6, blank gel matrix group (per day, NG).

CUMS Model Experiment

CUMS was used to replicate the rat model.[23] The specific stress methods were as follows: tail clamp (clamp applied 1 cm away from the end of the rat tail for 1 min), tilting the cage by 45° for 24 h, ice bath at 4°C for 5 min, day and night reversal for 24 h, fasting and water deprivation for 24 h, and exposure to noise for 12 h. One to two types of stress were randomly applied every day for 28 days; the weekly stress sequences are shown in Table 1.

After the modeling cycle, the rats were analyzed using the sucrose preference test (SPT), forced swimming test (FST), and box shuttle test (BST). Compared with the normal group, the forced swimming immobility time and escape latency significantly increased; the sucrose preference rate, movement, and exploration behavior were significantly reduced when the CUMS modeling was defined as successful.

SPT[23]

All the animals were trained to consume 1% sucrose. After fasting for 12 h, the rats were given 1% sucrose in a cage instead of drinking water. The rats were trained to consume sucrose for 1 h. The experiment was initiated after fasting for 2 h. During the test, two bottles with identical appearances (one containing purified water and the other containing 1% sucrose water) were placed in the rat cage. The weight difference of each bottle was recorded before and after 1 h, and the amount of sucrose water consumed was calculated.

Table 1 The Weekly Stress Sequence for Chronic Unpredictable Mild Stress (CUMS)

Groups	Day 1,8,15,22	Day 2,9,16,23	Day 3,10,17,24	Day 4,11,18,25	Day 5,12,19,26	Day 6,13,20,27	Day 7,14,21,28
Normal	Normal Feeding						
Model NG-Blank OANG-L OANG-H CH	Fasting for solids and liquids (24 h)	Forced swimming (15 min) andWet feeding (24 h)	The cage tilts 45° (24 h)	Binding test, (30min for each rats)	Day and night are reversed (24 h)	Ice bath at 4°C for 5 min and clip the tail (1 min for each rats).	Binding test, (30min for each rats)

Abbreviations: NG-blank, Thermosensitive gel without any drugs; OANG, Thermosensitive gel with OA Lipid cubic liquid crystal nanoparticles; CH, Clomipramine hydrochloride.

FST[24]

The experiments were conducted in a quiet environment. The swimming device was made of transparent plexiglass with a height of 40 cm, an inner diameter of 18 cm, a water depth of 30 cm, and a temperature of 25°C. Twenty-four hours before the experiment, rats were individually placed in the swimming device and forced to swim. After 15 min, the rats were removed from the water, dried with warm electric air, and returned to room temperature. During the formal experiment, a single rat was placed in the swimming device, slightly curled in the water, and allowed to float. The motionless behavior of the rat was considered immobile behavior, and the immobile time of the rat within 10 min was recorded. At the end of each test, the water in the swimming apparatus was replaced.

BST[25]

The test box was closed and divided by a partition into two chambers, A and B, connected through a door hole. The basic dimensions of the two chambers (L × W × H cm) were 50 × 36 × 32 cm, and the door hole was oval-shaped with dimensions (diameter × height cm) of 7.0×9.0 cm. During the test, a single rat was placed in the test box, and video tracking technology was used. The test lasted 15 min. The status of the animals in the test box was recognized, collected, analyzed, and automatically saved using the software.

Modified Neurologic Severity Scores (mNSS)

Rat neurological function was scored using the mNSS scale (Table 2). The degree of damage to neurological function positively correlated with the score, with higher scores indicating more severe injury. Specifically, a score of 0 indicated normal neurological function, 1 to 6 indicated mild impairment, 7 to 12 indicated moderate impairment, and 13 to 18 indicated severe impairment.[26]

Table 2 Modified Neurologic Severity Scores (mNSS)

Tests	Points
Motor tests	
Raising the rat by the tail	
Flexion of forelimb	1
Flexion of hindlimb	1
Head moving more than 10° (vertical axis)	1
Placing the rat on the floor	
Inability to walk straight	1
Circling toward the paretic side	1
Falling down to the paretic side	1
Sensory tests	
Visual and tactile placing	1
Proprioceptive test (deep sensory)	1
Beam balance tests	
Grasps side of beam	1
Hugs the beam and one limb falls down from the beam	2
Hugs the beam and two limbs fall down from the beam, or spins on beam (>60 s)	3
Attempts to balance on the beam but falls off (>40 s)	4
Attempts to balance on the beam but falls off (>20 s)	5
Falls off: no attempt to balance or hang on to the beam (<20 s)	6
Reflexes (blunt or sharp stimulation) absent of:	
Pinna reflex (a head shake when touching the auditory meatus)	1
Corneal reflex (an eye blink when lightly touching the cornea with cotton)	1
Startle reflex (a motor response to a brief loud paper noise)	1
Seizures, myoclonus, myodystony	1
Maximum points	18

Notes: One point is awarded for the exhibition of certain abnormal behavior or for the lack of a tested reflex. Score: 13–18 severe; 7–12 moderate; 1–6 mild injury.

https://doi.org/10.2147/DDDT.S484567

BNDF, AChE and Ach Determination

Brain tissue and blood samples were prepared as previously described. The levels of BDNF, AChE, and ACh in the brain tissues and hippocampus were determined using enzyme-linked immunosorbent assay (ELISA) according to the manufacturer's instructions.

IL-1β, IL-6 and 5-HT Determination

IL-1β and IL-6 concentrations in rat serum were determined using an ELISA kit. The content of the monoamine neurotransmitter 5-HT in the hippocampal homogenate was determined according to the ELISA kit instructions.

Network Pharmacological Analysis of the Anti-Depression Target Pathway of OA

Potential OA targets were searched on the Swiss Target platform, and depression-related targets were searched using the Online Mendelian Inheritance in Man (OMIM), DrugBank, and GeneCards databases.[27] The intersection of the two datasets was calculated using the "Venny 2.1" software. Disease-related targets involved in OA production were imported into the STRING database to obtain protein-protein interaction data. The species was set to "Homo sapiens" with the highest confidence > 0.9, and free nodes were deleted. All results were imported and analyzed using Cytoscape 3.7.1.

The intersecting genes were then imported into the DAVID database to identify key pathways for treating depression. The "Component-Target-Pathway" network diagram was constructed using Cytoscape 3.7.1, and Kyoto Encyclopedia of Genes and Genomes (KEGG) signal pathway enrichment analysis was performed on each node. "OFFICIAL GENE SYMBOL" was selected as the data model, and "Homo sapiens" was set as the species.

Brain Histopathological Examination

Fixed tissues were dehydrated using an automatic dehydrator, embedded, and sliced. The dewaxed sections were stained with hematoxylin and eosin (H&E), and histopathological conditions were observed under an optical microscope.

Data Processing and Statistical Analysis

All data are expressed as the mean ± standard deviation. One way analysis of variance (ANOVA) was performed using SPSS 21.0 to statistical analyze pharmacological parameters.

Results

In vitro Evaluation of Gels Loaded with OA-LCNP

Observation of Gelling Temperature and Condition

The results showed that an increase in F127 concentration decreased the critical temperature, consistent with the other test results (Figure 1B).[28] According to relevant research, water extruded by F127 micelles, which entangle with each other, is the driving force for gel formation.[29] Therefore, it is speculated that this is mainly due to the increase in F127 concentration, which increases the concentration of micelles generated at the same temperature. As a result, the water molecules extruded during micelle entanglement increase, making gel formation easier. In addition, F68 can reduce the critical temperature. The concentration screening results for F127 and F68 showed that when the F127 and F68 concentrations were 14%:6% and 13%:8%, respectively, the temperature requirements were met, and the liquid changed into a gel at 32 ± 1 °C (Figure 1A). Repeated tests were carried out with the above ratio, and it was found that when the dosage was increased, the ratio of F127 to F68 at 14%:6% was relatively stable In contrast, when the ratio was 13%:8%, the process varied, and sometimes the gel was formed at 28 °C. Therefore, a ratio of 14%:6% was selected for preparation. The prepared OANG was a flowing liquid at room temperature (25 °C) and successfully gelled when the temperature was increased to 34 °C (Figure 2A).

Rheological Study

The results showed that when the OA-LCNP was placed on the test table, flow occurred quickly. When the OANG was placed on the test table, no significant displacement occurred. As the temperature gradually decreased, the fluidity of OANG gradually increased, and friction with the table also gradually increased (Figure 1D).

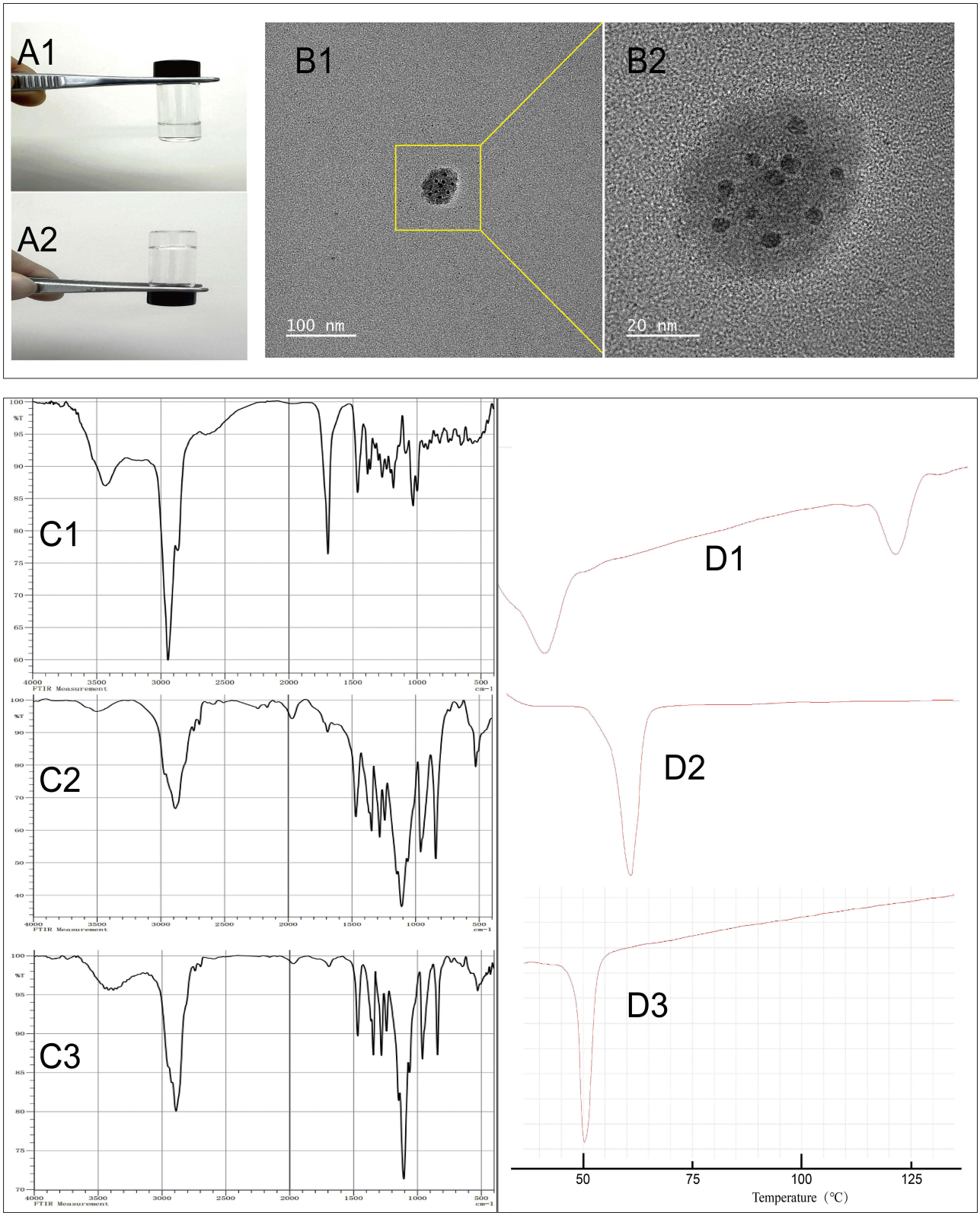

Figure 2 Results of morphological OANG characterization. (**A**) A1 - Gel appearance at 25°C; A2 - After warming at 34°C; (**B**) TEM results of gels loaded with OA-LCNP; (**C**) IR results: C1 - OA; C2 - Physical mixture of OA-LCNP, F127, and F68; C3 - OANG; (**D**) DSC results: D1 - OA; D2 - Physical mixture of OA-LCNP, F127, and F68; D3 - OANG.

https://doi.org/10.2147/DDDT.S484567

Drug Permeation Studies of OANG

The results of Franz diffusion experiments showed that OA-LCNP in the gel permeated more easily through rat skin and exhibited a slow release for up to 12 h. The zero-order, first-order, and Higuchi kinetic equations were used to analyze the in vitro permeation behavior of OA in temperature-sensitive gels (Table 3). The in vitro release curve of OANG conformed to the Higuchi kinetic equation (r = 0.9970), indicating that the drug release mechanism involved a synergistic effect on drug diffusion and skeleton dissolution. The results showed that the release of drugs during nasal administration was influenced by nasal fluid dissolution in the thermosensitive gel matrix and outward drug diffusion from the thermosensitive gel matrix.[30]

In vitro MTT Results

As shown in the figure, the survival rate of primary rat nasal mucosa cells on the OANG surface was 95%, and they gradually proliferated within 48 h (Figure 1E). Nasal mucosa cells with greater density grew vigorously and exhibited good cell vitality, indicating that OANG had no obvious toxic effects on primary rat nasal mucosa cells.

TEM Photographing

TEM results showed that the OA-LCNP were evenly dispersed in the gel, with an average particle size of 53 nm, where many OA-LCNP were distributed.

DSC Results

Figure 2 shows that OA has two melting point peaks at 35.6 °C and 117.5 °C, respectively. The physical mixture of OA, F127, and F68 had a melting point peak at 55 °C (D2). OANG had a melting point peak at 50.5 °C (D3). During the measurement process, F127 and F68 melted first, followed by the dissolution of OA in the carrier; therefore, the OA characteristic peak was not observed. The heat absorption peak of OANG is at 40 °C, and the melting point peak exists, which indicates that OANG is not a simple physical mixture formed with F127 and F68.[31]

IR Results

In the OA raw material, strong peaks were observed at 1700 cm^{-1}, 2960 cm^{-1}, and 3450 cm^{-1}, corresponding to the stretching vibrations of C=O, C-H, and -OH, respectively (Figure 2-C1). Both OA and the physical mixture (Figure 2-C1 and C2) showed absorption peaks at 3450 cm^{-1} and at approximately 1660 cm^{-1} and 1600 cm^{-1}. The O-H and C=O stretching vibrations of the physical mixture of OA and F127 can still be seen in the figure The infrared spectrogram results further showed that the OA physical mixture was only a simple superposition of the raw material and the carrier.[32]

Regarding OANG (Figure 2-C3), the intensity of the absorption peak at 3450 cm^{-1} significantly reduced, and the absorption peak became wider and blunter at 3470 cm^{-1}. The absorption peaks at 1736 cm^{-1} and 1664 cm^{-1} disappeared, suggesting hydrogen bond interaction between the drug and the carrier in OANG.[33]

Pharmacokinetic Results in Rats

Figure 3 shows the concentration-time curve results for OA in rat plasma and brain tissue. The main pharmacokinetic parameters and evaluation results for brain targeting are shown in Table 4. The area under the curve (AUC_{0-t}) of the brain tissue after nasal OANG administration was 1.21 times that after intravenous administration. Moreover, BTE and NDT were 29.91% and 9.44% higher than those after intravenous administration, respectively, indicating brain targeting by the OANG delivery system.

Table 3 Permeated Equation of OA-LCNP Thermosensitive Gel in vitro

Model	Permeated Equation	Correlation Coefficient (*r*)
Zero-order	$R = 31.08t + 24.16$	0.9844
First-order	$Ln(R) = 0.906Ln(t) + 3.829$	0.9798
Higuchi	$R = 141.9t^{\frac{1}{2}} - 99.64$	0.9970

Abbreviation: OA-LCNP, Oleanolic acid cubic liquid crystal nanoparticles.

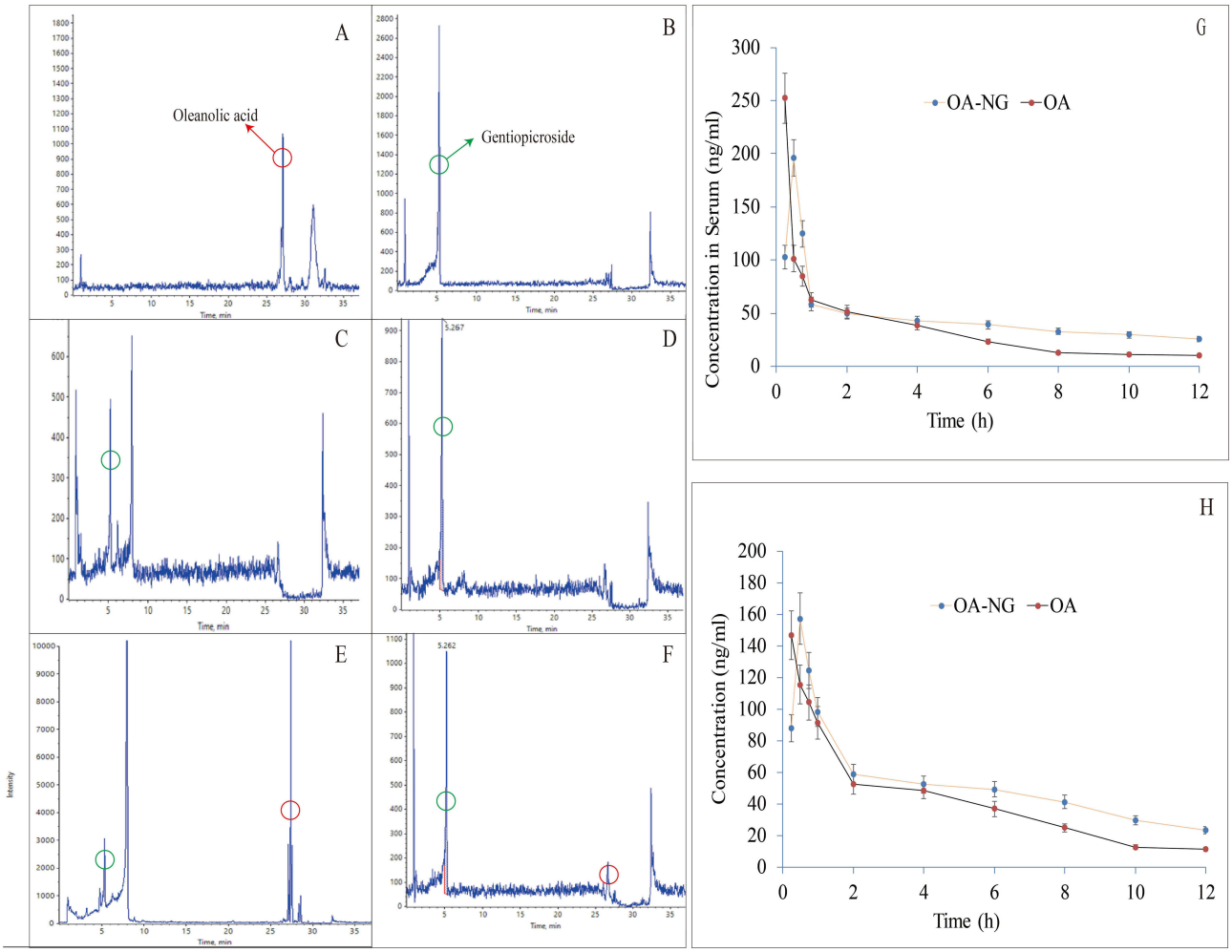

Figure 3 Results of rat pharmacokinetic experiments (n=5). (**A**–**E**) Mass spectrograms. (**A**) OA standard; (**B**) Gentiopicroside standard; (**C**) Blank serum with gentiopicroside added; (**D**) Medicated serum with gentiopicroside added; (**E**) Blank brain tissue with gentiopicroside added; (**F**) Medicated brain tissue with gentiopicroside added; (**G**) Time curve of OA concentration in serum; (**H**) Time curve of OA concentration in brain tissue.

The pharmacokinetic studies confirmed that OA encapsulation in OANG significantly improved the relative bioavailability to the brain, mean residence time (MRT), and OA half-life compared to the OA suspension ($p < 0.05$). The AUC (amount of drug absorbed by the brain) was also significantly higher (748.93 ± 62.38 ng·mL^{-1}·h^{-1}) compared with the OA suspension (618.78 ± 59.67 ng·mL^{-1}·h^{-1}) ($p < 0.05$).

CUMS Test Results in Rats

As shown in Figure 4A, when the rats were placed in a test box with a hole in the middle, curious rats typically passed through the hole to observe what was happening on the other side. When the rats were depressed, they were less curious about the outside world and naturally reduced the number of times they crossed the hole.[34] The instrument recorded the rat movements (Figure 4B).

Compared with the normal group, rat body weights in the model group significantly decreased during the 28-day CUMS test ($p < 0.05$, Figure 4C and D), probably due to fasting, water prohibition, and decreased appetite following various stimuli. The SPT results also showed that, compared with the normal group, the preference of the model rats for sugar significantly decreased ($p < 0.05$, Figure 4D). The FST results showed that the immobility time of the model group at 15 min was significantly higher than that of the normal group ($p < 0.05$, Figure 4E). The BST results showed that the number of box penetrations and active areas in the model group significantly decreased ($p < 0.05$, Figure 4F). Compared with the model group, no significant differences were observed in body weight, sugar water test results, immobility time

https://doi.org/10.2147/DDDT.S484567

Table 4 Main Pharmacokinetic Parameters for Oleanolic Acid ($\bar{x} + s$, n=5)

Parameters	Unit	OANG		OA (I.V.)	
		Serum	Brain	Serum	Brain
T_{max}	h	0.5	0.5	0.25	0.25
C_{max}	ng/mL	196.23±13.82	167.25±13.27	241.76±17.23	168.25±6.58
$t_{\frac{1}{2}}$	h	16.25±4.13	9.02±2.31*	19.05±2.36	8.93±0.92
$MRT_{0\sim t}$	h	7.63±0.49	7.64±0.32*	8.12±0.36	7.12±0.47
$AUC_{0\sim t}$	ng/(mL·h)	682.32±102.52	748.93±62.38*	728.39±84.24	618.78±59.67
BTE	%	129.21		100	
NDT	%	9.44		—	
F	%	93.68		100	

Note: *Statistical significance at p<0.01 when two groups compared.
Abbreviations: OA, Oleanolic acid; OANG, Thermosensitive gel of oleanolic acid Lipid with cubic liquid crystal nanoparticles; BTE, brain targeting efficiency; NDT, nasal-brain direct transfer; F, Absolute bioavailability.

in the FST, or penetration frequency in rats administered the blank gel, indicating that the blank gel had no therapeutic effect. Compared with the model group, in the OANG-H group, the body weight of the rats significantly increased ($p < 0.05$), preference for sugar water significantly increased ($p < 0.05$), immobility time in the FST significantly decreased ($p < 0.05$), and the number of box penetrations significantly increased ($p < 0.05$). No significant difference was observed between the experimental results and those of the positive control drug, CH ($p > 0.05$). Rat body weights in the OANG-L group significantly increased ($p < 0.05$). The results of the sugar water experiment showed that rat preference for sugar water significantly increased ($p < 0.05$), immobility time in the FST significantly decreased ($p < 0.05$), and the number of box penetrations significantly increased ($p < 0.05$).

As shown in Figure 5, no differences were observed between the blank gel and model groups in any of the indices ($p > 0.05$), indicating that the blank gel had no therapeutic effect on depression. Compared with the normal group, serum IL-4 and IL-6 levels were significantly higher in the model group than in the control group ($p < 0.05$, Figure 5A). Compared with the model group, serum IL-6 levels in the CH, OANG-L, and OANG-H groups were significantly lower ($p < 0.05$). Serum IL-4 levels in the CH group rats significantly decreased ($p < 0.05$). Serum IL-4 levels in the OANG-H and OANG-L groups did not significantly decrease ($p > 0.05$). Compared with the normal group, serum IL-1β levels in the model group significantly increased ($p < 0.05$, Figure 5B). Compared with the model group, serum IL-1β levels in the CH and OANG-H groups significantly decreased ($p < 0.05$). The serum IL-1β level in the OANG-L group did not significantly decrease ($p > 0.05$). The 5-HT content in the hippocampus of the model group significantly decreased ($p < 0.05$). Compared with the model group, 5-HT concentrations in rat hippocampus in the CH group were significantly higher ($p < 0.01$). The 5-HT content in rat hippocampus in the OANG-H and OANG-L groups significantly increased ($p < 0.05$). Compared with the normal group, the AChE content in rat serum and hippocampal tissue in the model group was significantly higher ($p < 0.05$, Figure 5C). AChE content in rat serum in the CH group and OANG-H group was significantly lower than in the model group ($p < 0.05$). The AChE content in the hippocampal tissue of the OANG-H group significantly decreased ($p < 0.01$). However, the AChE content in the hippocampal tissue of the OANG-L group did not significantly decrease ($p > 0.05$). Compared with the normal group, the ACh content in the hippocampus and serum of the model group was significantly lower ($p < 0.05$, Figure 5D). However, compared to the model group, the ACh content in rat serum and hippocampus in the CH, OANG-L, and OANG-H groups was significantly higher ($p < 0.05$).

Although some significant differences were observed in histological measurements, no significant differences were observed in behavioral scores by the mNSS test between the groups or between pre- and post-intervention (Figure 5E and F), probably due to the fact that rat behavioral scores have fewer indicators related to curiosity.[2]

Compared with the normal group, BDNF content in the rat hippocampus and serum in the model group was significantly decreased ($p < 0.05$, Figure 6A). Compared with the model group, the BDNF content in the rat hippocampus in the CH, OANG-L,

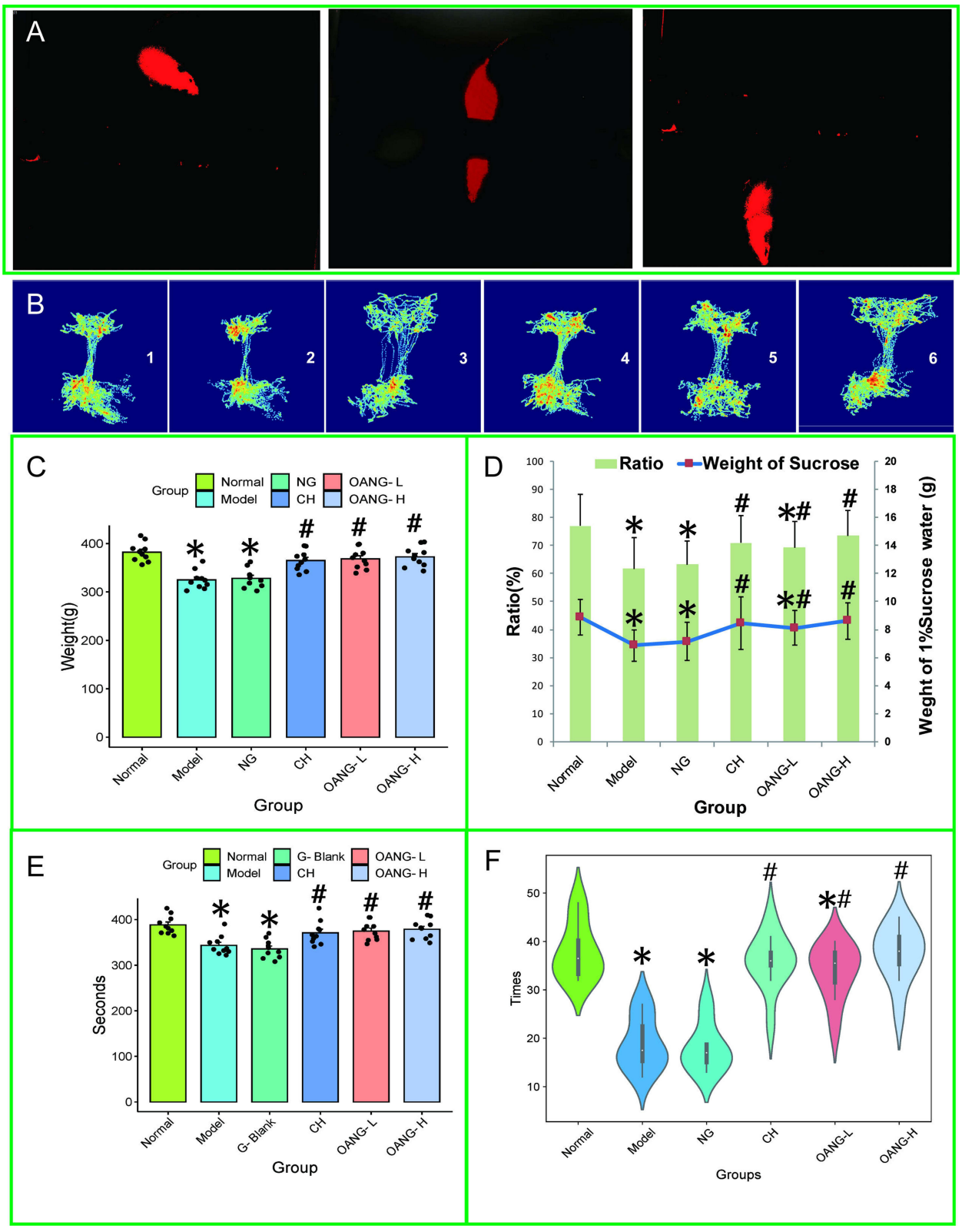

Figure 4 Results of CUMS test in rats (n=10). (**A**) Rats in the box shuttle test; (**B**) Shuttle track of rats: 1 - Normal, 2 - Model, 3 - NG, 4 - CH, 5 - OANG-L, and 6 - OANG-H groups; (**C**) Results of body weight comparison; (**D**) Results of sucrose preference tests; (**E**) Results of forced swimming tests; (**F**) Box shuttle test results. Comparison with the normal group, *$p < 0.05$; compared with the model group, #$p < 0.05$.

https://doi.org/10.2147/DDDT.S484567

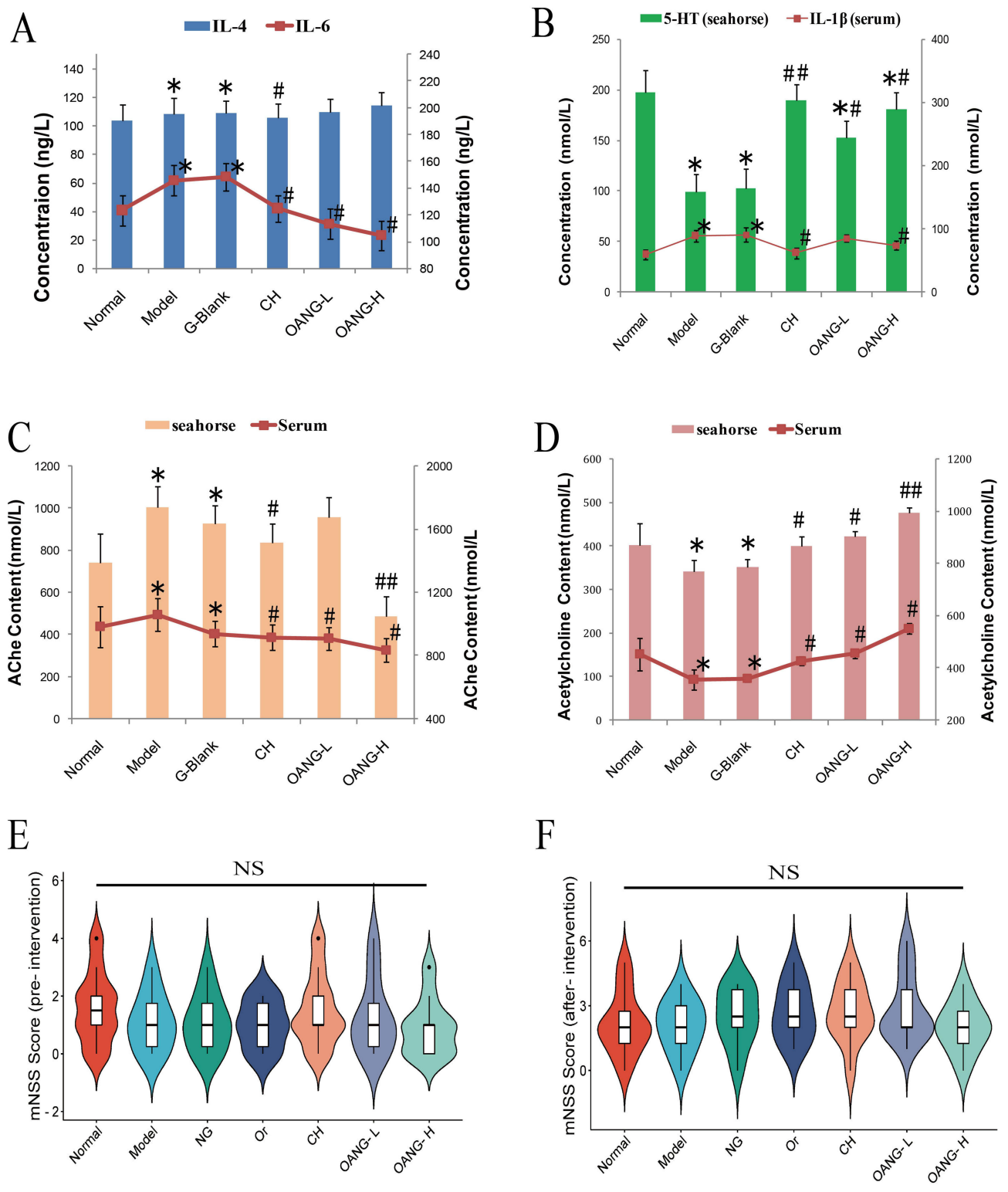

Figure 5 Pharmacological results in CUMS rats (n=10). (**A**) IL-4 and IL-6 concentration in rat serum; (**B**) 5-HT and IL-1β concentration in rat hippocampus and serum, respectively; (**C**) AChE concentration in rat hippocampus and serum; (**D**) Acetylcholine concentration in rat hippocampus and serum; (**E**) mNSS score (pre-intervention); (**F**) mNSS score (post-intervention). Comparison with the normal group, *$p < 0.05$; compared with the model group, $^{\#}p < 0.05$, $^{\#\#}p < 0.01$; NS means not significant ($p > 0.05$).

https://doi.org/10.2147/DDDT.S484567

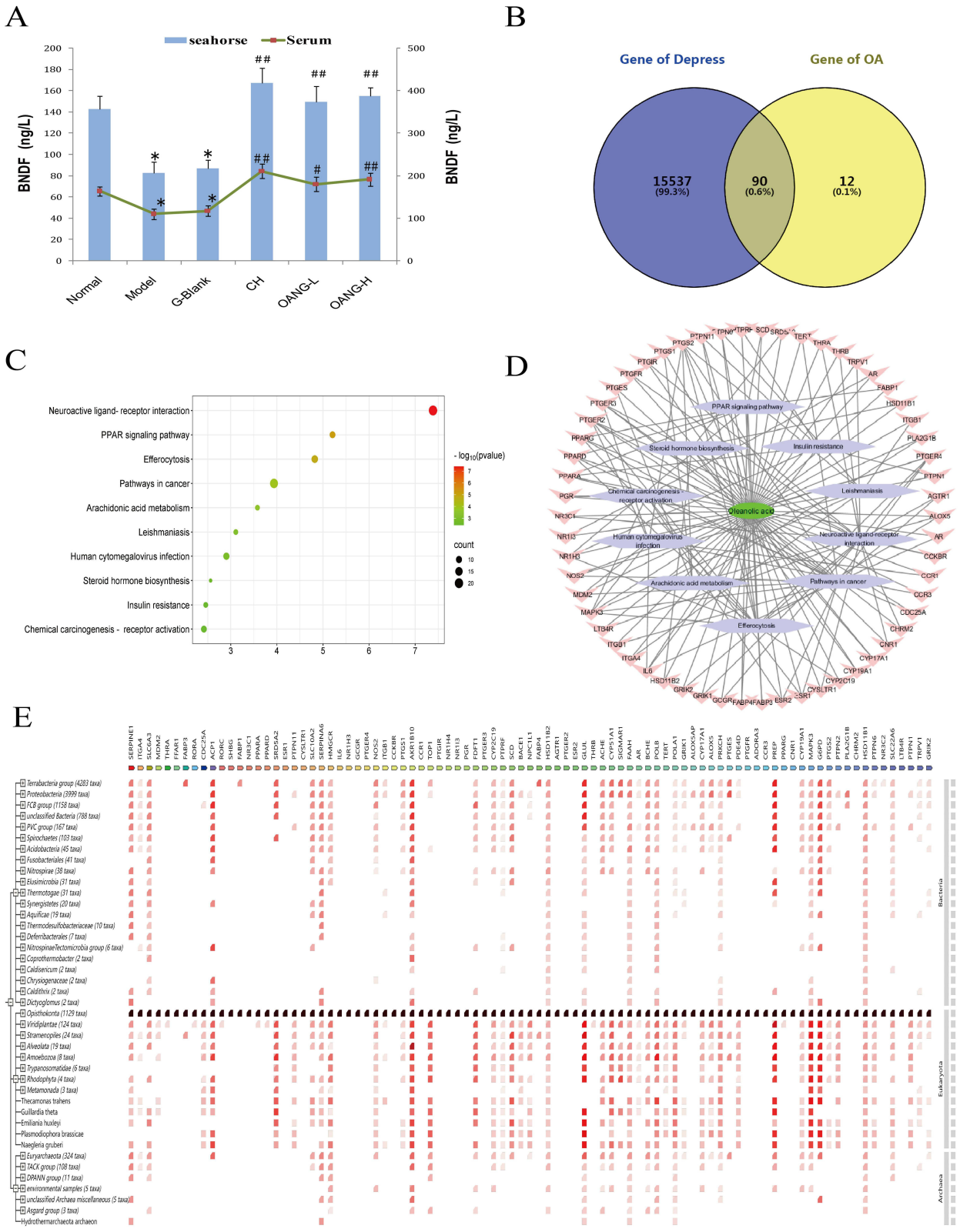

Figure 6 Results of pharmacological and network pharmacological analysis in CUMS rats (n=10). (**A**) BDNF concentration in rat hippocampus and serum; (**B**) Venn diagram of targets related to the pharmacological effects of depression and OA; (**C**) Bubble graph of signaling pathways in OA depression; (**D**) Graph of OA-target-signal pathway network; (**E**) STRING map of targets related to OA pharmacological effects on depression. Comparison with the normal group, *$p < 0.05$; compared with the model group, $^{\#}p < 0.05$, $^{\#\#}p < 0.01$.

https://doi.org/10.2147/DDDT.S484567

and OANG-H groups was significantly higher ($p < 0.01$). BDNF content in rat serum in the OANG-L group significantly increased ($p < 0.05$). BDNF content in the serum of the CH and OANG-H groups was significantly different ($p < 0.01$).

Network Pharmacological Analysis of the Anti-Depression Target Pathway of OA

The number of potential pharmacological targets of OA was 102 on the Swiss Target platform (http://www.swisstargetprediction.ch/), and 15,627 on OMIM (https://www.ncbi.nlm.nih.gov/omim), DrugBank (https://go.drugbank.com), and GeneCards (https://www.genecards.org/) online databases.[35] Ninety targets were found to be related to depression pharmacological effects, as shown in the Venn diagram (Figure 6B). The top ten potential signaling pathways for OA treatment of depression were calculated using KEGG, as shown in the bubble graph (Figure 6C). Intersecting genes were imported and analyzed using the STRING database (Figure 6D and E). The top three signaling pathways of OA in depression are neuroactive ligand-receptor interaction, peroxisome proliferator-activated receptor (PPAR) signaling pathway, and efferocytosis.

Histopathological Results

Normal group (Figure 7A): The tissue structure of the gray and white matter areas of the brain was normal, and the cell structure in the gray matter area was clear.[3] The pyramidal and granular cells were neatly arranged. The size, number, shape, and distribution of the cells were normal. The structures of the nucleus and cytoplasm were clear, and the color was uniform. The cytoplasm was light red, and the cell processes were visible. The nuclei were blue and clear, and the interstitial tissue was normal. Scattered glial cells were also observed.

Model and NG groups (Figure 7B and C): The tissue structures of the gray and white matter areas of the brain were normal. The number of cells in the gray matter area at the cellular level was normal. Mild edema of the cortical surface and pyramidal cells was observed.

CH group (Figure 7D): The tissue structures of the gray and white matter areas of the brain were normal. The cell structure in the gray matter area was clear. The pyramidal and granular cells were neatly arranged, and their size, number, shape, and distribution were normal. The nucleus and cytoplasm structures were clear, with a uniform color. The cytoplasm was light red, and the cell processes were visible. The nuclei were blue and clear. Mild edema of the pyramidal cells and mild inflammatory cell infiltration in the brain tissue were observed.

OANG-L and OANG-H groups (Figure 7E and F): The tissue structures of the gray and white matter areas of the brain were normal. The cell structure in the gray matter area was clear. The pyramidal and granular cells were neatly arranged, and their size, number, shape, and distribution were normal. The nucleus and cytoplasm structures were clear, and the color was uniform. The cytoplasm was light red, and the cell processes were visible. The nuclei were blue and clear, and no cone cell edema or inflammatory cell infiltration was observed.

Discussion

Nasal drug delivery has brain-targeting characteristics, bypassing the blood-brain barrier and rapidly reaching brain tissue.[21] It offers rapid absorption, quick onset of action, non-injury, convenient use, increased drug delivery to the brain, and higher drug concentrations in brain tissues. Enzyme activity is lower in the nasal cavity than in gastrointestinal digestive enzymes, which can effectively reduce drug metabolism, avoid the first-pass elimination effect, and improve drug bioavailability, achieving therapeutic effects.[36] OA is a triterpenoid compound isolated from Chinese herbal medicines that has anti-inflammatory and neuroprotective activities.[10,37] In addition, OA has been reported to be distributed in the rat brain following oral administration.[20] However, as an insoluble drug with low oral bioavailability, its brain tissue distribution is lower when orally administered, reducing its pharmacological effects. In a preliminary study, we prepared OA-LCNP to improve its oral bioavailability.[11]

Many methods for determining the gelling temperature have been reported, including magnetic stirring, viscosity measurements, and tube inversion.[38] This study used a uniformly sized mixer, with temperature and speed strictly and slowly controlled. When the mixer stopped rotating, the bottle was quickly turned upside down to measure the gel formation temperature. The combination of magnetic stirring and tube inversion has the advantages of being intuitive, simple to operate, and easy to control. It is expected that the temperature-sensitive gelation of the obtained preparation

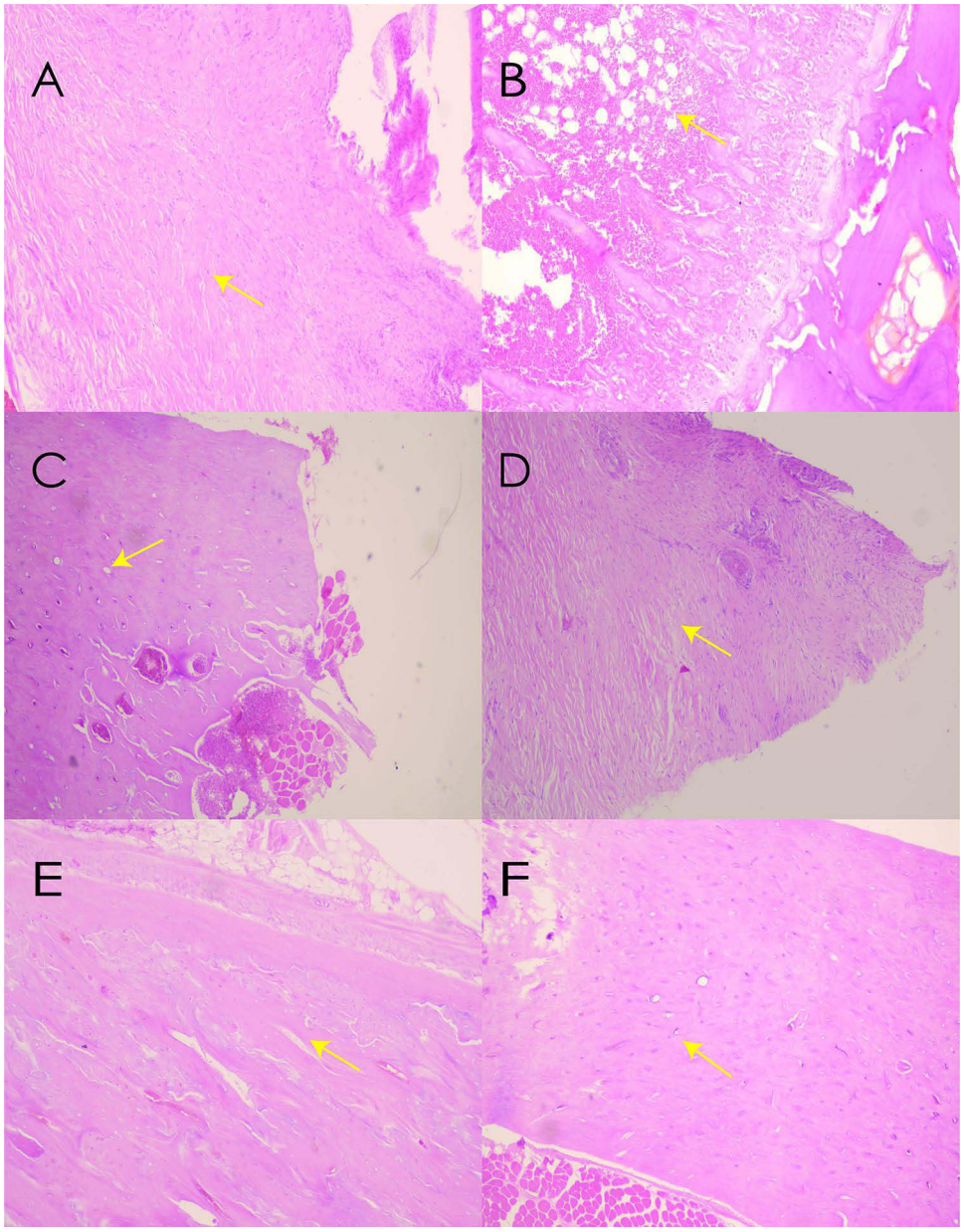

Figure 7 Pathological results of the brain in rats. (**A**) Normal, (**B**) Model, (**C**) NG, (**D**) CH, (**E**) OANG-L, and (**F**) OANG-H groups.

will occur rapidly when dropped into the nasal cavity. Studies have shown that the internal temperature of the normal human nasal cavity is 33–34°C, which was used as an evaluation index for prescription optimization.[39] F127 is the most commonly used substrate in thermosensitive gels, with the advantages of low toxicity and good biocompatibility, and was selected for OANG. However, because F127 alone cannot achieve the ideal gelling temperature, it may affect the gel's mechanical strength and dissolution rate. Thus, the prepared gel did not reach the desired effect expected from this experiment. The gelling temperature is related to the polyoxyethylene (PEO)/polyoxypropylene (PPO) block ratio in the polymer, and the gelling temperature decreases with increasing PPO content. The PEO/PPO block ratio of F68 is higher than that of F127; therefore, adding a small amount of F68 (0–6%) can alter the proportion of PEO/PPO blocks in the solution, increasing the gelling temperature, accelerating the gelling rate, enhancing gel adhesion, and reducing dissolution rates.[40] Therefore, F127 and F68 were simultaneously used as mixed substrates to prepare temperature-sensitive gels. In thermosensitive poloxamer gels, drug release occurs via two main mechanisms: dissolution and diffusion. The usual methods for measuring gel release in vitro include cell diffusion, dialysis bags, and non-membrane dissolution. In

https://doi.org/10.2147/DDDT.S484567

this study, the diffusion behavior of the gel was investigated in a diffusion cell. The release rates from the gel and aqueous solutions were measured under the same conditions. The results showed that the gel exhibited a slow-release effect.

Microglia are major participants in neuroinflammation and influence the expression of inflammation-related factors. Inflammatory factors associated with depression include IL-1β, IL-4, IL-6, and TNF-α.[41] Among these, the pro-inflammatory factors IL-1β, IL-4, and IL-6 are significantly upregulated in the hippocampus of model rats exposed to acute or chronic stressors.[34] The study found that when animals were exposed to acute and chronic stressors, an increase in IL-1β in the hippocampus inhibited hippocampal neurogenesis and induced depressive behavior. IL-6 also plays a role in the central nervous system of patients with depression, where it regulates monoamine metabolism, alters synaptic transmission in the brain, and reduces synaptic inhibition and excitation rates.[42,43] IL-4 is a multifunctional cytokine expressed in the brain.[44,45] It has been found that IL-4 maintains brain homeostasis, neuroprotection, and tissue repair by modulating microglia. The results showed that OANG administration effectively inhibited pro-inflammatory cytokine expression and promoted anti-inflammatory cytokine expression in the hippocampal tissues of model rats.[46]

As an important tryptophan metabolite, 5-HT is a neurotransmitter that induces positive emotions.[47] 5-HT is also involved in neuron production and the formation of neural circuits.[48] Studies have shown that 5-HT levels are significantly reduced in individuals with postpartum depression, which can lead to emotional and behavioral control disorders.[49] Abnormal serotonin metabolism is a classic mechanism underlying depression, and the anti-depressant chlorpromazine increases serotonin levels in the brain. In this study, we found that after 4 weeks of CUMS training in the model group, the 5-HT level in the hippocampus was significantly reduced. Both the low- and high-dose OANG groups showed increased 5-HT levels, which promoted recovery from depressive-like symptoms. In our previous experimental studies on OA and its anti-morphine addiction effects in rats, we found that the serum 5-HT content in morphine-addicted rats significantly decreased and that OA significantly increased the serum 5-HT levels.[50] Whether OA exerts a biphasic regulatory effect on 5-HT remains a topic for future studies.

The brain targeting of the drug can be preliminarily determined by comparing the value of AUC_{brain}/AUC_{serum} between nasal and intravenous administrations. If there is no nasal-brain pathway, the value of AUC_{brain}/AUC_{serum} after nasal administration should be lower than that after intravenous administration.[51,52] In this study, the OANG value was 1.10, higher than the 0.85 for intravenous administration, indicating that OANG had certain brain-targeting properties when administered through the nasal cavity. The AUC and MRT of intranasal OANG administration in brain tissue were significantly higher than those of intravenous OANG administration, indicating a longer mean retention time. Studies have shown that drugs that are not easily absorbed (such as proteins and peptides) are more likely to target the brain after nasal administration.[53] Although pharmacokinetic experiments were performed in two groups, only five samples were available at each time interval, and individual differences in rats may have influenced the experimental results.[54] Therefore, we did not perform statistical analyses of pharmacokinetic parameters between the two groups, such as ANOVA.[55,56] Preliminary results showed that BTE and NDT were 29.91% and 9.44% higher than those of intravenous administration, respectively, indicating brain targeting by the OANG delivery system.[57]

Neuronal structures can be altered in various ways, including dendrite retraction or extension, decreased or increased synaptic density (depending on the brain regions), and inhibited dentate gyrus neurogenesis.[58] Many intracellular and intercellular mediators are involved in these processes during the acute and recovery phases of stressful events, including BDNF, tissue plasminogen activator, corticotrophin- releasing factor, and Lipocalin-2. BDNF plays an important role in hippocampal dendrite remodeling.[59] Chronic stress induces BDNF downregulation in rats.[60] In this study, BDNF in the model group rats significantly decreased after 28 days of uncertain stimulation. Although the mechanism of BDNF alteration remains unclear, the BDNF-mediated signaling pathway is clearly involved in the structural effects of stress induction. The direction and nature of the signal are region-specific and stress-specific, and are affected by epigenetic and post-translational modifications.[61] Through network pharmacology studies, we found that depression is mainly treated through signaling pathways such as neuroactive ligand-receptor interaction, PPAR signaling pathway, and efferocytosis.[62] Studies have shown that OA exerts anti-inflammatory and pharmacological effects on microglial activation, cytokine levels, and IDO1 expression.[10] OA affects synaptic plasticity and resilience and has an even greater effect on depression-like behavior.[6] OA has been reported to improve synaptic plasticity of depression-like behaviors in

animal models. Studies have found that the cholinergic system in patients with depression and animal models involves changes in cholinesterase, acetyltransferase, and cholinergic receptors, which affect hippocampal synaptic plasticity and contribute to depression.[63] ACh, released by the ChAT transporter, plays a key role in neuronal excitability regulation throughout the brain.[64] ACh in the synaptic gap can be degraded by AChE, a key enzyme regulating extracellular ACh levels.[65,66] Further, in vivo experiments have shown that cholinergic activation can modulate bidirectional synaptic plasticity, and dopamine can reverse this.[67] Our study found that the ACh level in the hippocampus of depressed rats was upregulated, and that the OANG administration group could effectively reverse these effects and upregulate 5-HT levels, suggesting that OA may reverse synaptic inhibition through 5-HT and activate synapses through ACh to treat depression.

This study had some limitations. First, our findings were limited to CUMS model rats, and the etiology of depression is highly variable. In addition, clinical practice may not provide similar results. Therefore, OA's anti-depressant effects should be studied further in other depression models. Second, although changes in inflammatory factors such as 5-HT, BDNF, and IL-1β were observed in CUMS model rats, these protein levels may be altered due to changes in enzyme mRNA levels. Therefore, as a follow-up study, it is necessary to investigate the effects of OA administration on related amino acids and their metabolites in CUMS rats. Third, sex differences in neuroinflammation, synaptic plasticity, and the neuroendocrine system are thought to play an important role in the sex differences observed in mental disorders. For example, orexin expression is higher in female patients with depression than in male patients; moreover, differences exist in the sensitivity of the hypothalamic-pituitary-adrenal axis between female and male patients with depression.[68] Therefore, sex differences in the neuroendocrine aspects of OA treatment models for depression require further investigation.

Conclusion

In summary, our studies explored the OANG nasal drug delivery system has specific brain-targeting properties and can exert anti-depressant effects. Compared with traditional nano preparations, the composition of cubic liquid crystal nanoparticles is usually similar as the lipid composition of biofilm, and has a high affinity with nasal mucosa cells, which can not only reduce the irritation and damage to the nasal mucosa, but also increase the adhesion on the nasal mucosal surface, slow down the speed of clearance by the nasal mucus cilia, so that the drug can prolong the residence time in the nasal cavity. Therefore, the contact time between the drug and the nasal mucosa can be increased, and the absorption efficiency of the drug can be improved. In addition, the particle size of cubic liquid crystal nanoparticles is small, and it is easy to penetrate the nasal mucosa, and its special structure can regulate the drug release rate, which is conducive to the absorption of drugs across the nasal mucosa and improve the bioavailability of drugs. In this study, thermosensitive gel prepared with cubic liquid crystal nanoparticles as the matrix have good brain targeting properties.

Abbreviations

5-HT, 5-hydroxytryptamine (serotonin); ACh, acetylcholine; AChE, acetylcholinesterase; AUC, area under the curve; BDNF, brain-derived neurotrophic factor; BST, box shuttle test; CH, clomipramine hydrochloride; CRF, corticotropin-releasing factor; CUMS, chronic unpredictable mild stress; DAVID, database for annotation, visualization, and integrated discovery; DSC, differential scanning calorimetry; FST, forced swimming test; HPLC, high-performance liquid chromatography; IDOL, indoleamine 2,3-dioxygenase; IL-4, interleukin-4; IL-6, interleukin-6; IR, infrared spectroscopy; KEGG, Kyoto Encyclopedia of Genes and Genomes; LC-MS, liquid chromatography-mass spectrometry; LCNP, lipid cubic liquid crystal nanoparticles; MDD, major depressive disorder; mNSS, modified neurologic severity scores; NG, blank gel matrix per day; OA, oleanolic acid; OANG, OA-LCNP thermosensitive gel; OMIM, online Mendelian inheritance in man; PEG, polyethylene glycol; PPAR, peroxisome proliferator-activated receptor; SD, Sprague-Dawley (rats); SPT, sucrose preference test; TEM, transmission electron microscopy; TPA, tissue plasminogen activator; UPLC-MS/MS, ultra-performance liquid chromatography-tandem mass spectrometry.

Data Sharing Statement

All data generated or analyzed during this study are included in this published article.

Ethics Approval and Consent to Participate

The study was conducted in compliance with the ARRIVE guidelines. The experimental protocols and treatments were approved by the Ethics Committee of Wuxi Hospital of Traditional Chinese Medicine. All methods were performed in accordance with the Jiangsu Province Laboratory Animal Care and Use Guidelines.

Author Contributions

All authors made a significant contribution to the work reported, whether that is in the conception, study design, execution, acquisition of data, analysis and interpretation, or in all these areas; took part in drafting, revising or critically reviewing the article; gave final approval of the version to be published; have agreed on the journal to which the article has been submitted; and agree to be accountable for all aspects of the work.

Funding

This project was supported by the National Natural Science Foundation of China (Grant Number: 82274427), Top Talent Support Program for young and middle-aged people of Wuxi Health Committee (Grant Number: HB2023076), Taihu Talent Program for senior medical team project of Wuxi City (Grant Number: Talent Office of Wuxi [p2021] No.9), Traditional Chinese Medicine Bureau of Jiangsu Province and National Clinical base of Traditional Chinese Medicine open subject (Grant Number: JD2023SZ20), and Natural Science Foundation of Nanjing University of Traditional Chinese Medicine (Grant Number: XZR2023092).

Disclosure

The authors declare that they have no competing interests.

References

1. Wang C, Guo J, Guo R. Effect of XingPiJieYu decoction on spatial learning and memory and cAMP-PKA-CREB-BDNF pathway in rat model of depression through chronic unpredictable stress. *BMC Complement Altern Med*. 2017;17(1):73. doi:10.1186/s12906-016-1543-9
2. Ding K, Wang F, Wang K, et al. Environmental stress during adolescence promotes depression-like behavior and endocrine abnormalities in rats. *Behav Brain Res*. 2024;457:114710. doi:10.1016/j.bbr.2023.114710
3. Foudah AI, Alqarni MH, Alam A, Devi S, Salkini MA, Alam P. Rutin improves anxiety and reserpine-induced depression in rats. *Molecules*. 2022;27(21):7313. doi:10.3390/molecules27217313
4. Dudau L, Moisa E, Sevastre-Berghian A, et al. The effect of curcumin on reserpine-induced depression-like behaviour in rats. *Psychiatry Res*. 2023;334:111682. doi:10.1016/j.pscychresns.2023.111682
5. Castellano JM, Ramos-Romero S, Perona JS. Oleanolic acid: extraction, characterization and biological activity. *Nutrients*. 2022;14(3):623. doi:10.3390/nu14030623
6. Yi L, Li J, Liu Q, et al. Antidepressant-like effect of oleanolic acid in mice exposed to the repeated forced swimming test. *J Psychopharmacol*. 2013;27(5):459–468. doi:10.1177/0269881112467090
7. Dong SQ, Wang SS, Zhu JX, et al. Oleanolic acid decreases SGK1 in the hippocampus in corticosterone-induced mice. *Steroids*. 2019;149:108419. doi:10.1016/j.steroids.2019.05.011
8. Kong CH, Park K, Kim DY, et al. Effects of oleanolic acid and ursolic acid on depression-like behaviors induced by maternal separation in mice. *Eur J Pharmacol*. 2023;956:175954. doi:10.1016/j.ejphar.2023.175954
9. Yi LT, Li J, Liu BB, Luo L, Liu Q, Geng D. BDNF-ERK-CREB signalling mediates the role of miR-132 in the regulation of the effects of oleanolic acid in male mice. *J Psychiatr Neurosci*. 2014;39(5):348–359. doi:10.1503/jpn.130169
10. Liu J. Oleanolic acid and ursolic acid: research perspectives. *J Ethnopharmacol*. 2005;100(1–2):92–94. doi:10.1016/j.jep.2005.05.024
11. Shi Z, Pan S, Wang L, Li S. Topical gel-based nanoparticles for the controlled release of oleanolic acid: design and in vivo characterization of a cubic liquid crystalline anti-inflammatory drug. *BMC Complement Med*. 2021;21(1):255 doi:10.1186/s12906-021-03399-8.
12. Song J, Lu C, Leszek J, Zhang J. Design and development of nanomaterial-based drug carriers to overcome the blood-brain barrier by using different transport mechanisms. *Int J mol Sci*. 2021;22(18):10118. doi:10.3390/ijms221810118
13. Pawar GN, Parayath NN, Nocera AL, Bleier BS, Amiji MM. Direct CNS delivery of proteins using thermosensitive liposome-in-gel carrier by heterotopic mucosal engrafting. *PLoS One*. 2018;13(12):e208122. doi:10.1371/journal.pone.0208122
14. Morgese G, Trachsel L, Romio M, Divandari M, Ramakrishna SN, Benetti EM. Topological polymer chemistry enters surface science: linear versus cyclic polymer brushes. *Angew Chem Int Ed*. 2016;55(50):15583–15588. doi:10.1002/anie.201607309
15. Marquele-Oliveira F, Torres EC, Barud HDS, et al. Physicochemical characterization by AFM, FT-IR and DSC and biological assays of a promising antileishmania delivery system loaded with a natural Brazilian product. *J Pharmaceut Biomed*. 2016;123:195–204. doi:10.1016/j.jpba.2016.01.045
16. Zhang W, Chen J, Gu J, et al. Nano-carrier for gene delivery and bioimaging based on pentaetheylenehexamine modified carbon dots. *J Colloid Interf Sci*. 2023;639:180–192. doi:10.1016/j.jcis.2023.02.046
17. Vedadghavami A, Zhang C, Bajpayee AG. Overcoming negatively charged tissue barriers: drug delivery using cationic peptides and proteins. *Nano Today*. 2020;34:100898. doi:10.1016/j.nantod.2020.100898

18. Zhang X, Ning F, Li Y, et al. Pluripotent polysaccharide coordinated hydrogels remodel inflammation, neovascularization and reepithelization for efficient diabetic wound prohealing. *J Control Release*. 2025;377:37–53. doi:10.1016/j.jconrel.2024.11.027
19. Pailla S, Sampathi S, Junnuthula V, Maddukuri S, Dodoala S, Dyawanapelly S. Brain-targeted intranasal delivery of zotepine microemulsion: pharmacokinetics and pharmacodynamics. *Pharmaceutics*. 2022;14(5):978. doi:10.3390/pharmaceutics14050978
20. Jeong DW, Kim YH, Kim HH, et al. Dose-linear pharmacokinetics of oleanolic acid after intravenous and oral administration in rats. *Biopharm Drug Dispos*. 2007;28(2):51–57. doi:10.1002/bdd.530
21. Khan AR, Liu M, Khan MW, Zhai G. Progress in brain targeting drug delivery system by nasal route. *J Control Release*. 2017;268:364–389. doi:10.1016/j.jconrel.2017.09.001
22. Mohammadi P, Mahjub R, Mohammadi M, Derakhshandeh K, Ghaleiha A, Mahboobian MM. Pharmacokinetics and brain distribution studies of perphenazine-loaded solid lipid nanoparticles. *Drug Dev Ind Pharm*. 2021;47(1):146–152. doi:10.1080/03639045.2020.1862172
23. Hong C, Chen L, Kong W, et al. Behavioral and neurochemical changes in rats with recurrent depression induced by chronic unpredictable stress. *Neuroendocrinol Lett*. 2021;42(6):387–394.
24. Arauchi R, Hashioka S, Tsuchie K, et al. Gunn rats with glial activation in the hippocampus show prolonged immobility time in the forced swimming test and tail suspension test. *Brain Behav*. 2018;8(8):e1028. doi:10.1002/brb3.1028
25. Chen S, Asakawa T, Ding S, et al. Chaihu-Shugan-San administration ameliorates perimenopausal anxiety and depression in rats. *PLoS One*. 2013;8(8):e72428. doi:10.1371/journal.pone.0072428
26. Naghdi M, Ghovvati M, Rabiee N, et al. Magnetic nanocomposites for biomedical applications. *Adv Colloid Interfac*. 2022;308:102771. doi:10.1016/j.cis.2022.102771
27. Liu T, Shao Q, Wang W, et al. Integrating network pharmacology and experimental validation to decipher the mechanism of the Chinese herbal prescription JieZe-1 in protecting against HSV-2 infection. *Pharm Biol*. 2022;60(1):451–466. doi:10.1080/13880209.2022.2038209
28. Salatin S, Barar J, Barzegar-Jalali M, Adibkia K, Milani MA, Jelvehgari M. Hydrogel nanoparticles and nanocomposites for nasal drug/vaccine delivery. *Arch Pharm Res*. 2016;39(9):1181–1192. doi:10.1007/s12272-016-0782-0
29. Gu F, Fan H, Cong Z, Li S, Wang Y, Wu C. Preparation, characterization, and in vivo pharmacokinetics of thermosensitive in situ nasal gel of donepezil hydrochloride. *Acta Pharm*. 2020;70(3):411–422. doi:10.2478/acph-2020-0032
30. Mathure D, Sutar AD, Ranpise H, Pawar A, Awasthi R. Preparation and optimization of liposome containing thermosensitive in situ nasal hydrogel system for brain delivery of sumatriptan succinate. *Assay Drug Dev Technol*. 2023;21(1):3–16. doi:10.1089/adt.2022.088
31. Nakahashi-Ouchida R, Yuki Y, Kiyono H. Cationic pullulan nanogel as a safe and effective nasal vaccine delivery system for respiratory infectious diseases. *Hum Vaccine Immunother*. 2018;14(9):2189–2193. doi:10.1080/21645515.2018.1461298
32. Luo S, Zhao Y, Pan K, et al. Microneedle-mediated delivery of MIL-100(Fe) as a tumor microenvironment-responsive biodegradable nanoplatform for O2 -evolving chemophototherapy. *Biomater Sci*. 2021;9(20):6772–6786. doi:10.1039/D1BM00888A
33. Song Y, Cong Y, Wang B, Zhang N. Applications of Fourier transform infrared spectroscopy to pharmaceutical preparations. *Expert Opin Drug Deliv*. 2020;17(4):551–571. doi:10.1080/17425247.2020.1737671
34. Malhi GS, Mann JJ. Depression. *Lancet*. 2018;392(10161):2299–2312. doi:10.1016/S0140-6736(18)31948-2
35. Liu T, Chen W, Chen X, et al. Network pharmacology identifies the mechanisms of action of TaohongSiwu decoction against essential hypertension. *Med Sci Monit*. 2020;26:e920682 doi:10.12659/MSM.920682.
36. Pardridge WM. The blood-brain barrier: bottleneck in brain drug development. *NeuroRx*. 2005;2(1):3–14. doi:10.1602/neurorx.2.1.3
37. Singh GB, Singh S, Bani S, Gupta BD, Banerjee SK. Anti-inflammatory activity of oleanolic acid in rats and mice. *J Pharm Pharmacol*. 1992;44 (5):456–458. doi:10.1111/j.2042-7158.1992.tb03646.x
38. Zhong Y, Su C, Wu S, Miao C, Wang B. Nasal delivery of an immunotherapeutic vaccine in thermosensitive hydrogel against allergic asthma. *Int Immunopharmacol*. 2023;116:109718. doi:10.1016/j.intimp.2023.109718
39. Sridhar V, Wairkar S, Gaud R, Bajaj A, Meshram P. Brain targeted delivery of mucoadhesive thermosensitive nasal gel of selegiline hydrochloride for treatment of Parkinson's disease. *J Drug Target*. 2018;26(2):150–161. doi:10.1080/1061186X.2017.1350858
40. Wang Q, Zuo Z, Cheung CKC, Leung SSY. Updates on thermosensitive hydrogel for nasal, ocular and cutaneous delivery. *Int J Pharmaceut*. 2019;559:86–101. doi:10.1016/j.ijpharm.2019.01.030
41. Kurata K, Nagasawa M, Tomonaga S, et al. Orally administered l-ornithine reduces restraint stress-induced activation of the hypothalamic-pituitary-adrenal axis in mice. *Neurosci Lett*. 2012;506(2):287–291 doi:10.1016/j.neulet.2011.11.024.
42. Kelly KM, Smith JA, Mezuk B. Depression and interleukin-6 signaling: a Mendelian randomization study. *Brain Behav Immun*. 2021;95:106–114. doi:10.1016/j.bbi.2021.02.019
43. Ting EY, Yang AC, Tsai S. Role of Interleukin-6 in Depressive Disorder. *Int J mol Sci*. 2020;21(6):2194. doi:10.3390/ijms21062194
44. Perry BI, Upthegrove R, Kappelmann N, Jones PB, Burgess S, Khandaker GM. Associations of immunological proteins/traits with schizophrenia, major depression and bipolar disorder: a bi-directional two-sample Mendelian randomization study. *Brain Behav Immun*. 2021;97:176–185. doi:10.1016/j.bbi.2021.07.009
45. Ge PY, Qu SY, Ni SJ, et al. Berberine ameliorates depression-like behavior in CUMS mice by activating TPH1 and inhibiting IDO1 associated with tryptophan metabolism. *Phytother Res*. 2023;37(1):342–357. doi:10.1002/ptr.7616
46. Ogłodek E. Changes in the serum levels of cytokines: IL-1β, IL-4, IL-8 and IL-10 in depression with and without posttraumatic stress disorder. *Brain Sci*. 2022;12(3):387. doi:10.3390/brainsci12030387
47. Yohn CN, Gergues MM, Samuels BA. The role of 5-HT receptors in depression. *mol Brain*. 2017;10(1):28. doi:10.1186/s13041-017-0306-y
48. Borroto-Escuela DO, Ambrogini P, Chruścicka B, et al. The role of central serotonin neurons and 5-HT heteroreceptor complexes in the pathophysiology of depression: a historical perspective and future prospects. *Int J mol Sci*. 2021;22(4):1927. doi:10.3390/ijms22041927
49. Popova NK, Tsybko AS, Naumenko VS. The implication of 5-HT receptor family members in aggression, depression and suicide: similarity and difference. *Int J mol Sci*. 2022;23(15):8814. doi:10.3390/ijms23158814
50. Shi Z, Pan S, Wang L, Li S. Oleanolic acid attenuates morphine withdrawal symptoms in rodents: association with regulation of dopamine function. *Drug Des Devel Ther*. 2021;15:3685–3696. doi:10.2147/DDDT.S326583
51. Yang Y, Huang H, Cui Z, Chu J, Du G. UPLC-MS/MS and network pharmacology-based analysis of bioactive anti-depression compounds in betel nut. *Drug Des Devel Ther*. 2021;15:4827–4836. doi:10.2147/DDDT.S335312

52. Yin P, Han X, Yu L, et al. Pharmacokinetic analysis for simultaneous quantification of Saikosaponin A- paeoniflorin in normal and poststroke depression rats: a comparative study. *J Pharmaceut Biomed*. 2023;233:115485. doi:10.1016/j.jpba.2023.115485
53. Miziak B, Czuczwar SJ, Pluta R. Comorbid epilepsy and depression—pharmacokinetic and pharmacodynamic drug interactions. *Front Pharmacol*. 2022;13:988716. doi:10.3389/fphar.2022.988716
54. Neuhäuser M, Jöckel K. A bootstrap test for the analysis of microarray experiments with a very small number of replications. *Appl Bioinformatics*. 2006;5(3):173. doi:10.2165/00822942-200605030-00005
55. Fieberg JR, Vitense K, Johnson DH. Resampling-based methods for biologists. *PEERJ*. 2020;8:e9089 doi:10.7717/peerj.9089.
56. Panos GD, Boeckler FM. Statistical analysis in clinical and experimental medical research: simplified guidance for authors and reviewers. *Drug Des Devel Ther*. 2023;17:1959–1961. doi:10.2147/DDDT.S427470
57. Lee JH, Ji SH, Lim JS, et al. Anti-neuroinflammatory effects and brain pharmacokinetic properties of selonsertib, an apoptosis signal-regulating kinase 1 inhibitor, in mice. *Neurochem Res*. 2022;47(12):3829–3837. doi:10.1007/s11064-022-03777-9
58. Zhang X, Wang L, Xiong L, Huang F, Xue H. Timosaponin B-III exhibits antidepressive activity in a mouse model of postpartum depression by the regulation of inflammatory cytokines, BNDF signaling and synaptic plasticity. *Exp Ther Med*. 2017;14(4):3856–3861. doi:10.3892/etm.2017.4930
59. Molendijk ML, Spinhoven P, Polak M, Bus BAA, Penninx BWJH, Elzinga BM. Serum BDNF concentrations as peripheral manifestations of depression: evidence from a systematic review and meta-analyses on 179 associations (N = 9484). *mol Psychiatry*. 2014;19(7):791–800. doi:10.1038/mp.2013.105
60. Xin C, Xia J, Liu Y, Zhang Y. MicroRNA-202-3p targets brain-derived neurotrophic factor and is involved in depression-like behaviors. *Neuropsych Dis Treat*. 2020;16:1073–1083.
61. Murawska-Ciałowicz E, Wiatr M, Ciałowicz M, et al. BDNF impact on biological markers of depression-role of physical exercise and training. *Int J Environ Res Public Health*. 2021;18(14):7553. doi:10.3390/ijerph18147553
62. Zhang T, Wei W, Chang S, Liu N, Li H. Integrated network pharmacology and comprehensive bioinformatics identifying the mechanisms and molecular targets of Yizhiqingxin formula for treatment of comorbidity with Alzheimer's disease and depression. *Front Pharmacol*. 2022;13:853375. doi:10.3389/fphar.2022.853375
63. Gao J, Lai M, Fu W, et al. Electroacupuncture ameliorates depressive-like state and synaptic deficits induced by hyper-cholinergic tone during chronic stress in rats. *Med Sci Monit*. 2021;27:e933833 doi:10.12659/MSM.933833.
64. Prior C, Singh S. Factors influencing the low-frequency associated nicotinic ACh autoreceptor-mediated depression of ACh release from rat motor nerve terminals. *Brit J Pharmacol*. 2000;129(6):1067–1074. doi:10.1038/sj.bjp.0703161
65. Ning B, Wang Z, He J, et al. The rapid antidepressant effect of acupuncture on two animal models of depression by inhibiting M1-Ach receptors regulates synaptic plasticity in the prefrontal cortex. *Brain Res*. 2024;1822:148609. doi:10.1016/j.brainres.2023.148609
66. Gargouri B, Bouchard M, Saliba SW, et al. Repeated bifenthrin exposure alters hippocampal Nurr-1/AChE and induces depression-like behavior in adult rats. *Behav Brain Res*. 2019;370:111898. doi:10.1016/j.bbr.2019.04.012
67. Mineur YS, Mose TN, Blakeman S, Picciotto MR. Hippocampal α7 nicotinic ACh receptors contribute to modulation of depression-like behaviour in C57BL/6J mice. *Brit J Pharmacol*. 2018;175(11):1903–1914. doi:10.1111/bph.13769
68. Ziemichód W, Kurowska A, Grabowska K, Kurowska M, Biała G. Characteristics of Seltorexant-innovative agent targeting Orexin system for the treatment of depression and anxiety. *Molecules*. 2023;28(8):3575. doi:10.3390/molecules28083575